Nature Environment and Pollution Technology
An International Quarterly Scientific Journal

p-ISSN: 0972-6268
(Print copies up to 2016)
e-ISSN: 2395-3454

Vol. 21 | No. 3 | pp. 1357-1365 | 2022

Original Research Paper

https://doi.org/10.46488/NEPT.2022.v21i03.043

Open Access Journal

Study on Adsorption Properties and Mechanism of Graphene Oxide (GO) by Kaolin

Xingjiang Song*, Lin Zhou, Haibo Kang**†, Na Li**, Wei Wang** and Ping Jiang****

*Anhui and Huaihe River Water Resources Research Institute, Bengbu, China

**School of Civil Engineering, Shaoxing University, Shaoxing, Zhejiang, P. R. China

†Correspondence author: Haibo Kang; 18020852079@usx.edu.cn

Nat. Env. & Poll. Tech.
Website: www.neptjournal.com

Received: 30-07-2021
Revised: 04-10-2021
Accepted: 05-10-2021

Key Words:
Graphene oxide
Kaolin
Adsorption properties
Adsorption mechanism

ABSTRACT

Kaolin was used as an adsorbent to remove toxic graphene oxide (GO) from an aqueous solution. The adsorption properties and mechanism of GO by Kaolin were systematically studied by various characterization techniques and methods. The effects of pH, amount of absorbent, and initial concentration of GO on the adsorption of GO by Kaolin were studied in detail. The results show that the interaction between GO and Kaolin is realized by the O-C=O bond, and the adsorption of GO by Kaolin is a chemical adsorption process. Under the optimized conditions (pH=3, T=303 K, equilibrium time = 6 h, C_0 = 60 mg·L^{-1}), the removal rate of GO reached 97.1% (Kaolin=70 mg), and the adsorption capacity reached 45.3 mg·g^{-1} (Kaolin=50 mg). According to the experimental results, Kaolin may be a promising material, which can effectively eliminate GO from an aqueous solution. The results of this study provide key information about the migration and potential fate of GO in the natural environment.

INTRODUCTION

Since its discovery, graphene oxide (GO) has attracted worldwide attention due to its unique structure and remarkable physical and chemical properties. GO shows great potential in multidisciplinary fields, such as medical treatment, energy, environmental pollution control, etc. (Azadian et al. 2019, Baragao et al. 2020, Jing et al. 2019). Specifically, due to its high specific surface area and excellent structural convertibility, a series of GO-based nanomaterials have been used in wastewater treatment (Awad et al. 2018, İlayda et al. 2016, Xing et al. 2019). For example, GO was used as an adsorbent to remove sulfamethoxazole and ciprofloxacin from an aqueous solution successfully (Chen et al. 2015). Magnetic graphene/iron oxide composite was used for the removal of U(VI) from an aqueous solution by Zong et al. (2013). GO nanosheets treated with Fe_3O_4 nanoparticles were used for simultaneous removal of Cu (II) and fulvic acid from an aqueous solution (Li et al. 2012). To effectively remove as (III) and (V), nano-sized zero valiant iron reduced graphite oxide composites were prepared (Wang et al. 2014). GO/pyrrole composites can remove phenol and aniline from an aqueous solution (Hu et al. 2015).

Although GO and GO-based nanomaterials have been widely used as adsorbents for environmental pollution cleaning, GO is inevitably released into the environment and ecosystem, including surface water and groundwater (Qi et al. 2014b). Accordingly, due to the toxicity of GO, more and more attention has been paid to the transport of GO and its negative impact on the environment. Many studies have shown that GO is toxic to organisms, including bacterial cells and human beings (Chowdhury et al. 2013). For example, Akhavan and Ghaderi (Akhavan & Ghaderi 2010) found that GO particles reduced the viability of staphylococcus aureus and Escherichia coli due to their sharp edges. In addition, GO can also produce cytotoxicity to human skin fibroblasts and HeLa cells (Liao et al. 2011). Besides, GO can cause high lung accumulation and long-term retention, which may lead to many lung diseases (Vallabani et al. 2011, Zhang et al. 2011). Once GO is released into the natural environment, it may threaten human health because of its nanostructure and toxicity. Therefore, it is necessary to remove GO from the natural aquatic environment, in which it is very important to understand its physical and chemical behavior.

In recent years, various types of natural clays and modified clays, such as Kaolin (Al-Degs et al. 2014), Tunisian montmorillonite (Wiem et al. 2018), sodium montmorillonite (Haouti et al. 2019), silica bentonite (Queiroga et al. 2019), polyamide vermiculite nanocomposites (Basaleh et al. 2019) and lithium feldspar clay sodium alginate composite materials (Pawar et al. 2018) have been used to remove ions, dyes, and heavy metals from the water environment.

Using natural clay as an alternative adsorbent to remove dyes from wastewater has the advantages of low cost, high adsorption performance, high porosity, good usability, good thermal stability, great ion-exchange potential, and non-toxicity (Bao et al. 2019, Puri & Sumana 2018). In this regard, Kaolin is one of the well-known rich and low-cost natural clays, which have crystalline structures all over the world (Yavuz & Saka 2013). Generally speaking, Kaolin is mainly composed of Kaolinite and some minerals such as quartz and mica (Vimonses et al. 2009). The surface of Kaolinite has a constant structural negative charge, which is due to the isomorphic substitution of Si^{+4} by Al^{+3} in the silicon layer. It is considered an active adsorption site for removing harmful substances from wastewater, which depends on the pH value of the solution (He et al. 2019, Mouni et al. 2017, Nandi et al. 2009). These characteristics cast kaolin high adsorption, kaolin adsorption of metal ions more research results, the adsorption capacity of Pb (II) is 118.5mg·g-1, (Nguyen et al. 2021), The highest adsorption rate can reach 85.1% (Hussain & Ali 2021).

There are few studies on the use of Kaolin as an adsorbent to remove GO in water environments at home and abroad (Mouni et al. 2017, Kryuchkova & Fakhrullin 2018). The adsorption behavior of GO by Kaolin was studied systematically. Specifically, Kaolin and GO before and after adsorption were characterized by SEM, TEM, XRD, FT-IR, and AFM for their microscopic morphology, lattice structure, and surface functional groups. The effects of pH value, the initial concentration of GO, and the amount of adsorbent on the adsorption performance were studied and evaluated in detail. Finally, XPS was used to study the difference between bond energy before and after adsorption, and the mechanism of interaction between Kaolin and GO was proposed. This work attempts to provide a new idea for the development of high-efficiency sorbents for capturing GO in the environment.

MATERIALS AND METHODS

Experimental Materials

Graphene aqueous solution (2 $mg.mL^{-1}$) was used as the source of GO, and graphene aqueous solution was purchased from Suzhou Carbon Technology Co., Ltd. Kaolin (1250 mesh) was used as an adsorbent, which was purchased from Shanghai Beimo Industrial Co., Ltd. The chemical constituents of Kaolin are shown in Table 1. 0.1 $mol.L^{-1}$ NaOH solution and 0.1 $mol.L^{-1}$ HCl solution were all analytically pure reagents.

Feature Description

The crystal structure of the absorbent was studied by X-ray diffraction (XRD). The functional groups were identified by Fourier transform infrared spectroscopy (FT-IR, NEXUS). The infrared scanning range was 400-4000 cm^{-1}. Scanning electron microscopy (SEM, JSM-6360LV), Atomic force microscopy (AFM, SPA400), and High-resolution transmission electron microscopy (HRTEM, JEM-2100f) were used to study the morphology and structure of the materials before and after adsorption. X-ray photoelectron spectroscopy (XPS) analysis was performed by focusing a monochromatic Alka X-ray source (hm=1486.6eV) with Thermo ESCALAB250.

Adsorption Experiment

First, an appropriate amount of GO solution was poured into a 50 mL container. Then, a certain amount of adsorbent was added in turn for the batch adsorption test. Afterward, the container was placed in an ultrasonic cleaner at a certain temperature for 30 min. Next, the container was put into a constant temperature shaker for 1 h under shaking to ensure the adsorption process. After the shaking is completed, it was left to stand for 12 h to make the reaction complete. Finally, 1 mL supernatant of the reaction solution was extracted and diluted to 25.0 mL. The residual GO concentration in the supernatant was analyzed at 210 nm wavelength by UV visible spectrophotometer (UV1800).

Different factors (Initial pH value of GO solution, concentration of GO solution, and amount of adsorbent) were optimized. First, when the temperature was 303 K and the GO concentration on the simulated aqueous solution was 60 $mg{\cdot}L^{-1}$, the initial pH of the GO solution (3.0-8.0) was changed and the amount of adsorbent was 50 mg. Second, when the temperature was 303 K, the initial pH of the GO solution was 3, and the initial GO concentration was 60 $mg{\cdot}L^{-1}$, the mass of the adsorbent (30-70 mg) was changed. Finally, when the temperature was 303 K, the initial pH of the GO solution was 3, and the amount of adsorbent was 70 mg, the experiment was carried out by changing the concentration of GO in an aqueous solution (20 $mg{\cdot}L^{-1}$-100 $mg{\cdot}L^{-1}$). Results of the optimized parameters of adsorption

Table 1: Chemical constituents of Kaolin.

SiO_2 (%)	Al_2O_3 (%)	Fe_2O_3 (%)	TiO_2 (%)	CaO (%)	MgO (%)	K_2O (%)	Na_2O (%)	MnO (%)
52±2	45±2	<0.4	<1.0	<0.4	<0.2	<0.04	<0.1	<0.005

conditions were obtained. To ensure the accuracy and repeatability of the collected data, all experiments were repeated 3 times, and the average value of the three experiments was used as the follow-up data analysis. The removal percentage ($R\%$), adsorption capacity (Q_e), and partition coefficient (K_d) were used to evaluate the adsorption performance of Kaolin. The adsorption capacity (Q_e) represents the amount of GO adsorbed on the adsorbent per unit weight. The following equation (Eq) is used to calculate the relevant parameters (Eq.1-3) (Zou et al. 2016).:

$$R = \frac{C_0 - C_e}{C_0} \times 100\% \quad \ldots(1)$$

$$Q_e = \frac{(C_0 - C_e) \times V}{\mathrm{m}} \quad \ldots(2)$$

$$K_d = \frac{Q_\mathrm{e}}{C_e} \quad \ldots(3)$$

Where C_0 (m·L^{-1}) is the initial GO concentration of an aqueous solution, and C_e (mg·L^{-1}) is the equilibrium GO concentration. m (g) is the amount of adsorbent and V (L) is the volume of solution. K_d is the distribution coefficient.

RESULTS AND DISCUSSION

Effect of pH

The pH value of GO solution is an important parameter for adsorption, not only because the distribution of GO in water mainly depends on the pH value of the solution, but also because the surface of the adsorbent can be protonated or deprotonated. Therefore, the effects of pH on the adsorption capacity, removal rate, and partition coefficient were investigated by adjusting the pH value of the solution. In fact, under other conditions (Adsorbent amount 50 mg, C_0 = 60 mg·L^{-1}, equilibrium time 6 h, T = 303 K), the pH value was optimized in the range of 3.0-8.0. The results are shown in Fig. 1. It can be seen from the figure that when pH = 3, Kaolin adsorbs more than 75% of GO. On the one hand, it may be that under acidic pH, GO has a strong self-aggregation ability (Konkena & Vasudevan 2012), resulting in a small amount of GO suspended in the solution. On the other hand, GO and Kaolin are an electrostatic attraction at this time, so the interaction ability is strong, the GO in the supernatant is very small and the adsorption rate is very high. The adsorption capacity of GO by Kaolin decreases with the increase of pH in the range of 3-8. When pH = 8, the adsorption capacity is almost zero. This may be due to the weakening of electrostatic interaction between Kaolin and GO with the increase of pH value. It should be noted that there is electrostatic repulsion between kaolin and GO in the pH range of 3.0-8.0, so the adsorption in this process may be chemical. That is the hydrogen bond interaction and Lewis acid-base interaction between the oxygen-containing functional groups on the surface of GO and the oxygen-containing groups on the mineral surface (Qi et al. 2014a, He et al. 2019, Mouni et al. 2017, Nandi et al. 2009).

Therefore, it can be concluded that a low pH value is conducive to the adsorption of GO by Kaolin, and alkaline conditions will inhibit the adsorption of GO by Kaolin. It

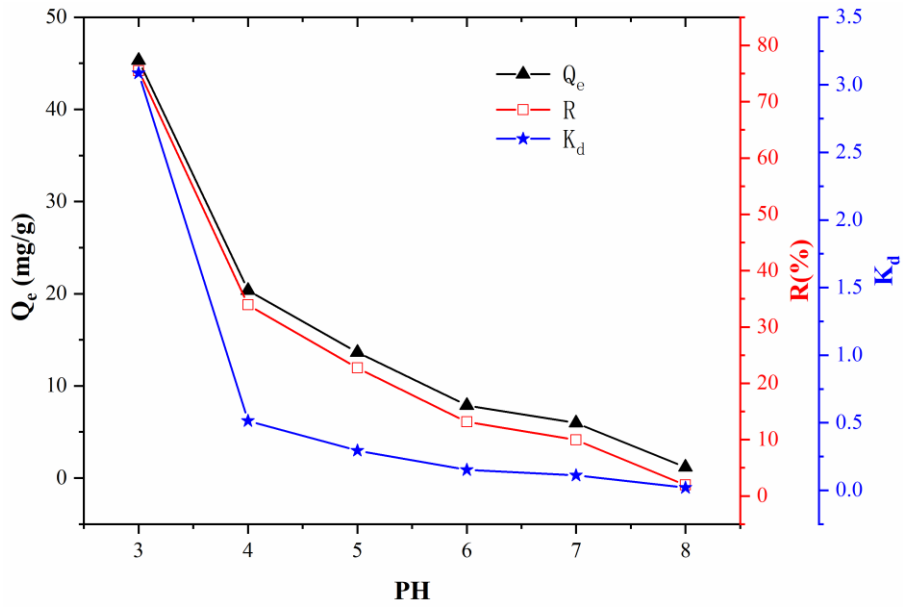

Fig. 1: Removal of GO by Kaolin as a function of pH value.

is suggested that the adsorption process should be carried out at pH = 3.

Effect of Adsorbent Mass

The amount of adsorbent is also one of the important parameters affecting the removal of harmful substances in an aqueous solution. Therefore, the influence of Kaolin contents on adsorption capacity, removal rate, and partition coefficient was investigated by changing the amount of Kaolin. In fact, under other conditions (Adsorbent mass pH = 3, C_0 = 60 mg·L^{-1}, equilibrium time 6 h, T = 303 K), the Kaolin content was optimized in the range of 30 mg-70 mg. Fig. 2 shows the effect of Kaolin content on the adsorption capacity, efficiency, and partition coefficient. It can be seen from the figure that the removal rates increase with the increase in Kaolin content. When the Kaolin content is 70 mg, the removal rate is close to 100%. Similarly, the adsorption capacity and distribution coefficient also reach the maximum value. The results show that with the increase in Kaolin content, the adsorption sites of Kaolin and GO increase, which makes Kaolin have high adsorption capacity and can better remove GO from aqueous solution, thus playing an important role in the application of Kaolin to remove GO from aqueous solution.

Effect of GO Initial Concentration

The initial concentration of GO is also an important parameter affecting the removal of GO by Kaolin. Therefore, the effects of GO initial concentration on adsorption capacity, removal rate, and partition coefficient were investigated by changing the initial concentration of GO. In fact, under other conditions (Adsorbent mass pH = 3, Kaolin content = 70 mg, equilibrium time 6 h, T = 303 K), the initial GO concentration was optimized in the range of 20 mg·L^{-1}-100 mg·L^{-1}. Fig.3 shows the effect of GO initial concentration on adsorption capacity, efficiency, and partition coefficient. It can be seen from the figure that with the increase of GO initial concentration, the removal first increases and then decreases. When the GO initial concentration is 60 mg·L^{-1}, the removal rate is close to 100%. The results show that the adsorption sites and electrostatic interaction between Kaolin and GO increase with the increase of GO concentration when the initial GO concentration is 20 mg·L^{-1}-60 mg·L^{-1}. When the initial GO concentration is 60 mg·L^{-1}-100 mg·L^{-1}, the increase in GO concentration inhibits the electrostatic interaction between Kaolin and GO, resulting in a decrease in the GO removal rate (Zou et al. 2016, Wang et al. 2016).

Therefore, when Kaolin is used to remove GO from water solution, the concentration of GO in aqueous solution should be measured first, to achieve the best effect of removing GO by Kaolin.

SEM and TEM Analysis

Fig. 4 shows SEM (a) and TEM (b) of GO and SEM (c) and TEM (d) of Kaolin /GO. It can be seen that the SEM images of GO are multi-layer lamellar three-dimensional structures, and the SEM images of Kaolin/GO also show lamellar structures.

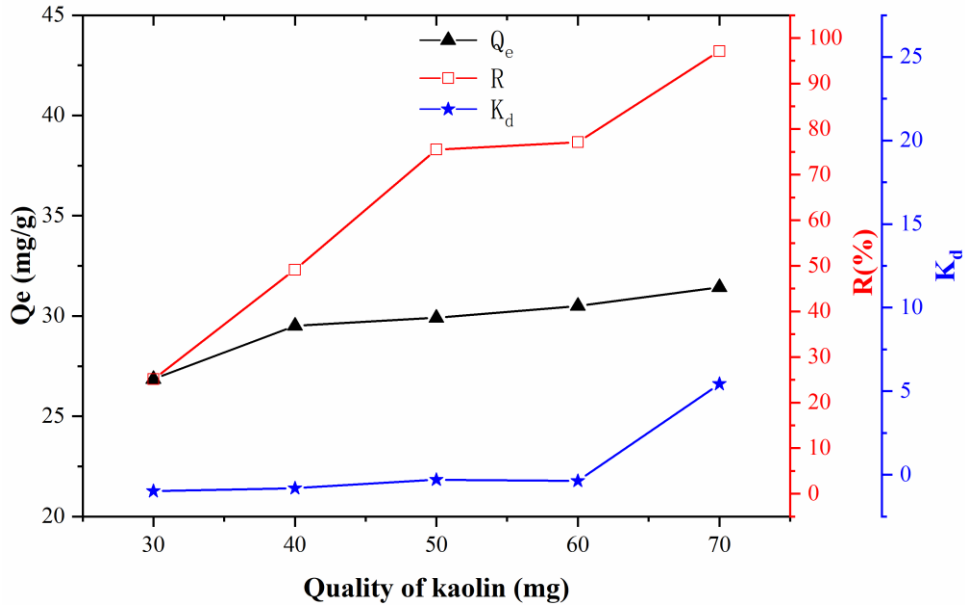

Fig. 2: Removal of GO by Kaolin as a function of Kaolin contents.

This indicates that GO is adsorbed on Kaolin. The comparison between the TEM (b) diagram of GO and the TEM (d) diagram of Kaolin/GO can also reveal this phenomenon, which proves that Kaolin can remove GO from water solution.

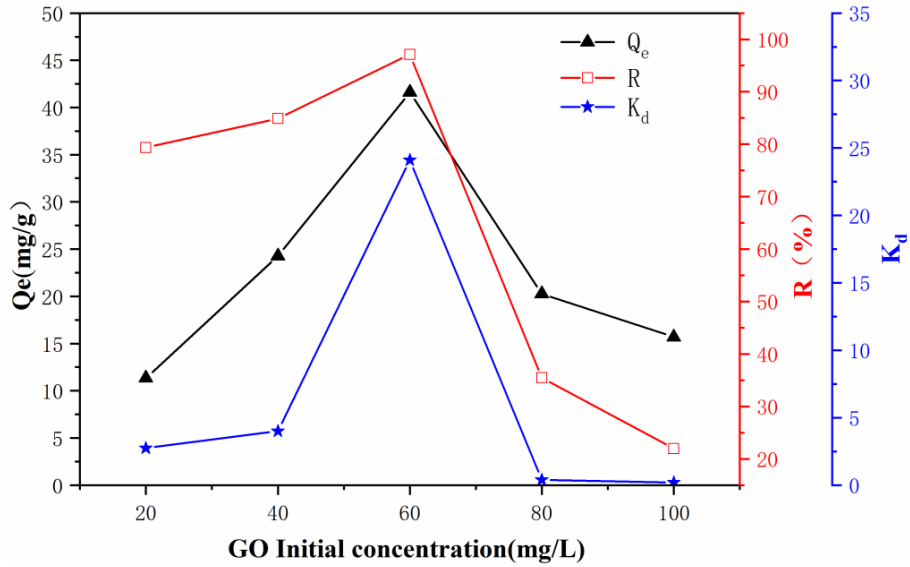

Fig. 3: Removal of GO by Kaolin as a function of GO contents.

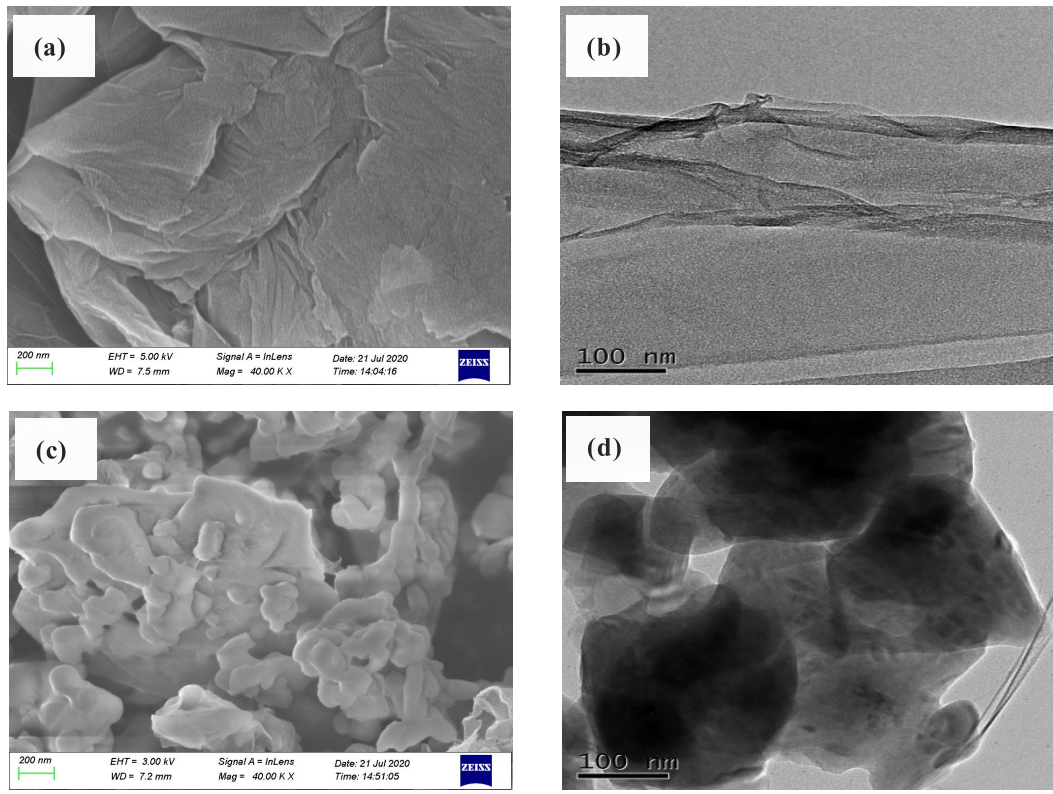

Fig. 4: SEM (a) and TEM (b) of GO, SEM (c) and TEM (d) of Kaolin/GO.

XRD and FT-IR Analysis

To reveal the adsorption mechanism, GO, Kaolin, and Kaolin/GO materials were characterized by XRD technology, and the results are shown in Fig. 5(a). It can be seen from the figure that the characteristic diffraction peaks of Kaolin/GO and Kaolin are almost the same, which indicates that GO is not accumulated on the surface of Kaolin but wrapped in Kaolin. This is consistent with the results of TEM and SEM of Kaolin/GO.

For the sake of obtaining the effective adsorption functional groups of Kaolin surface before and after GO adsorption, FT-IR analysis was carried out. Fig. 5(b) shows the FT-IR spectra of GO, Kaolin, and Kaolin after adsorption of GO. The main band on FT-IR of Kaolin at ~3448 cm^{-1} can be attributed to the tensile vibration of O-H, while the frequency band of ~1635 cm^{-1} can be attributed to the bending vibration of coordination water (Deng & Shi 2015, Mouni et al. 2017). The peaks at ~1110 cm^{-1} and ~990 cm^{-1} can be attributed

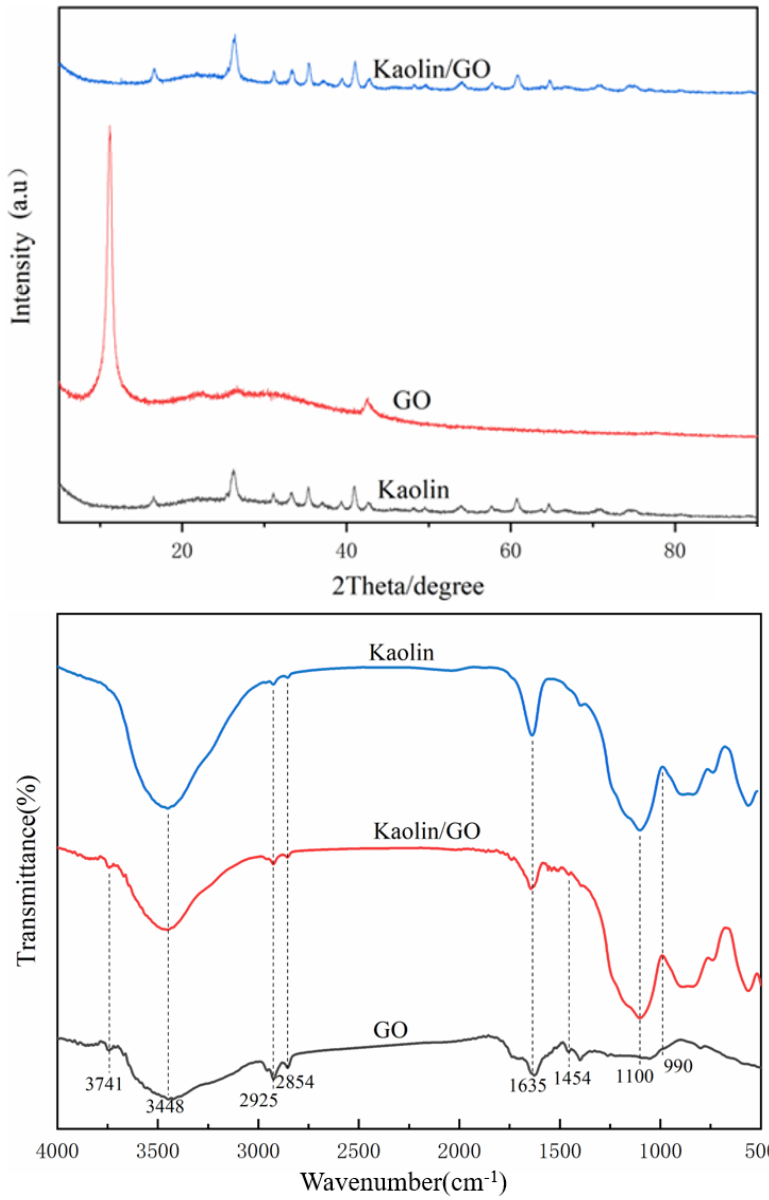

Fig. 5: XRD patterns (a) of GO, Kaolin, Kaolin/GO, FT-IR patterns (b) of GO, Kaolin, Kaolin/GO.

to the tensile vibration of Si-O-Si of Kaolinite (Mouni et al. 2017). The FT-IR spectra of Kaolin after adsorption of GO showed that the functional groups of Kaolin participated in the adsorption of GO. In addition, a new band appears at ~1484cm^{-1}, which may be due to the (C = C) of GO adsorbed on the Kaolin surface. A new band appears at ~3741cm^{-1}, which is the same as that of GO.

XPS and AFM Analysis

To further explore the adsorption mechanism of GO by Kaolin, GO and Kaolin/GO were analyzed by XPS and AFM. The results are shown in Fig. 6 and Fig. 7, respectively. As shown in Fig. 6(a), various strong peaks, such as Al2p, Si2p, N1, S2p, O1s, and C1s can be observed. According to the high-resolution spectrum of C1s before adsorption of GO, the deconvolution of the C1s spectrum can be divided into three components, about 284.7 eV, 286.7 eV, and 288.5 eV, respectively, which are assigned to C-C, C-O, and O-C=O groups (Fig. 6(b)) (Littunen et al. 2011, Yu et al. 2012, Zhang et al. 2014). However, after Kaolin adsorbs GO, the intensity and position of C1s peak of Kaolin/GO change. The relative areas of C-C, C-O, and O-C=O assigned to Kaolin/GO decrease significantly, and the peak position of O-C=O changes from 288.5 eV to 288.8 eV. The peak positions of C-C and C-O are almost unchanged (Fig. 6(c)). The relative area and peak position of O-C=O changes obviously, which indicates that the interaction between GO and Kaolin is carried out by O-C=O. From the height of the AFM image and the corresponding morphology, the thickness of GO is 1.02 nm, and the thickness of Kaolin/GO is 2.55 nm, which indicates that the thickness of Kaolin/GO becomes thicker due to the aggregation of GO in Kaolin, which is consistent with TEM results. Based on the above analysis, Kaolin can effectively remove GO through the aggregation of GO in Kaolin.

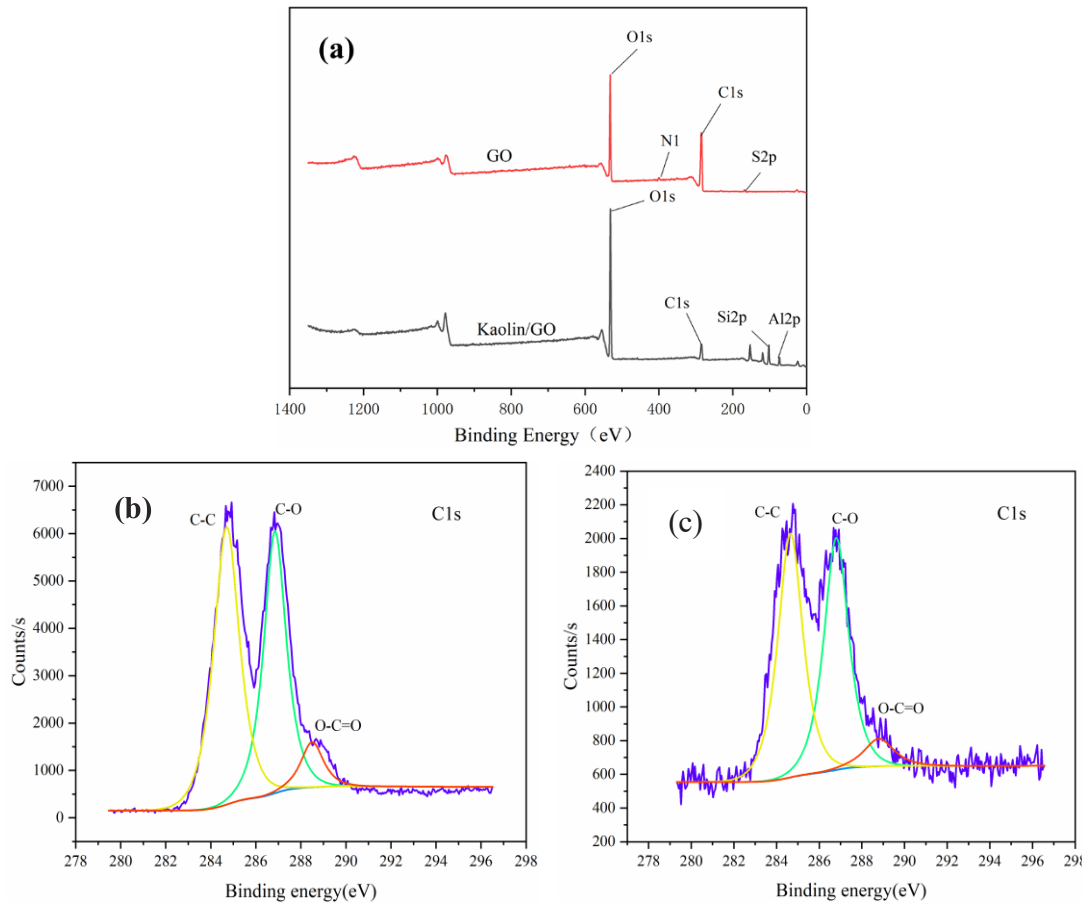

Fig. 6: XPS spectra of Kaolin/GO before and after GO removal (a), the high C1s deconvolution of GO (b), and the high C1s deconvolution of Kaolin/GO (c).

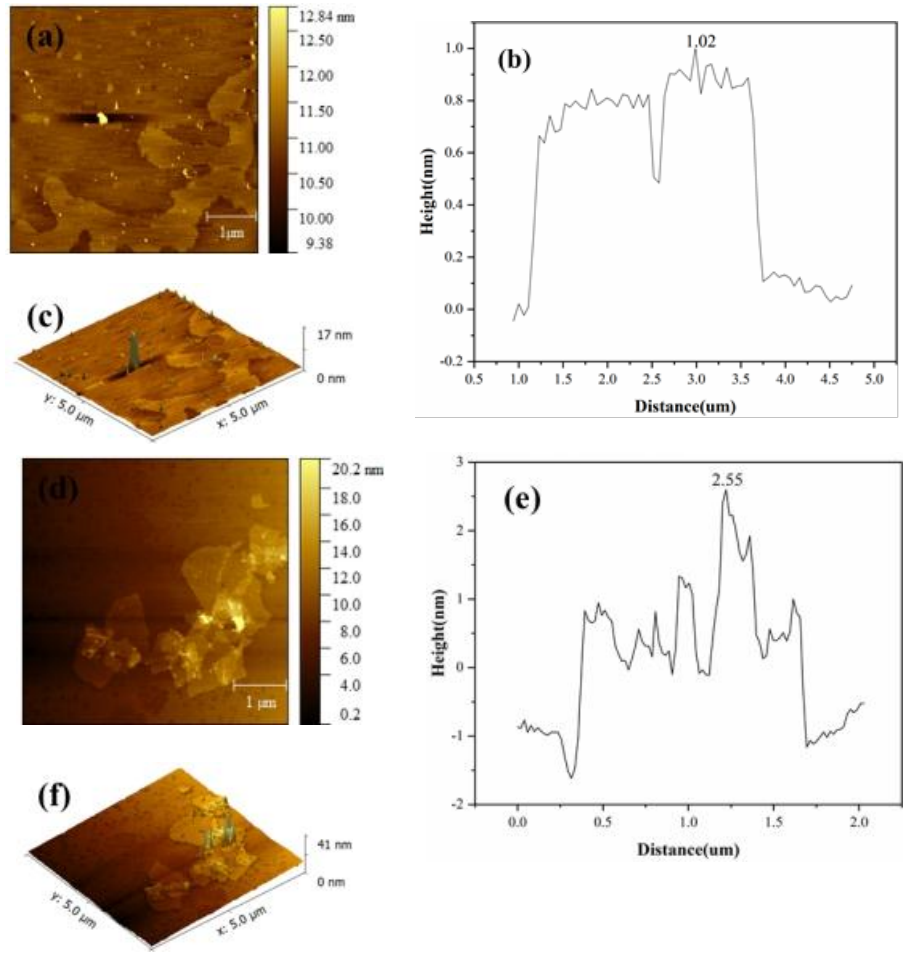

Fig. 7: AFM image and the corresponding height profiles of GO (a) (b) (c) and Kao/GO (d) (e) (f).

CONCLUSION

This paper studies the kaolin's adsorption performance and mechanism of GO and has obtained some meaningful conclusions: The highest removal rate and adsorption capacity was 97.1%, and 45.3 mg, respectively. The microscopic characterization further confirmed the occurrence of the Human Soil in the GO adsorption process, where the XPS spectrum showed the interaction of GO and kaolin was achieved by the O-C=O key, and kaolin's adsorption of GO was a chemical adsorption process. In summary, kaolin can effectively remove GO in an aqueous solution by simple and rapid chemical adsorption.

ACKNOWLEDGMENT

This research was funded by the National Natural Science Foundation of China (52179107). Thanks to Weiqing Zhang and Jiahui Gu for assistance with the experiments.

REFERENCES

Akhavan, O. and Ghaderi, E. 2010. Toxicity of graphene and graphene oxide nanowalls against bacteria. ACS Nano, 4(10): 5731-5736.

Al-Degs, Y.S., Al-Ghouti, M.A. and Olimat, A.A.M. 2014. Studying competitive sorption behavior of methylene blue and malachite green using multivariate calibration. Chem. Eng. J., 11: 251.

Awad, F.S., Abouzied, K.M., Abou, E.M., El-Wakil, A.M. and Samy, E.S.M. 2018. Effective removal of mercury(II) from aqueous solutions by chemically modified graphene oxide nanosheets. Arab. J. Chem., 13: 2659-2670.

Azadian, E., Arjmand, B., Ardeshirylajimi, A., Hosseinzadeh, S. and Khojasteh, A. 2019. Polyvinyl alcohol modified polyvinylidene fluoride raphene oxide scaffold promotes osteogenic differentiation potential of human-induced pluripotent stem cells. J. Cell. Biochem., 121(5-6).

Bao, T., Damtie, M.M., Wu, K., Wei, X.L., Zhang, Y., Chen, J., Deng, C.X., Jin, J., Yu, Z.M. and Wang, L. 2019. Rectorite-supported nano-Fe3O4 composite materials as a catalyst for P-chlorophenol degradation: Preparation, characterization, and mechanism. Appl. Clay Sci., 176(8): 66-77.

Baragao, D., Forján, R., Welte, L. and Gallego, J.L.R. 2020. Nanoremediation of As and metals polluted soils by means of graphene oxide nanoparticles. Sci. Rep., 10(1): 54.

Basaleh, A., Al-Malack, M.H. and Saleh, T.A. 2019. Methylene Blue removal using polyamide-vermiculite nanocomposites: Kinetics, equilibrium and thermodynamic study. J. Environ. Chem. Eng., 7(3): 43.

Chen, H., Gao, B. and Li, H. 2015. Removal of sulfamethoxazole and ciprofloxacin from aqueous solutions by graphene oxide. J. Hazard. Mater., 282(23): 201-207.

Chowdhury, I., Duch, M.C., Mansukhani, N.D., Hersam, M.C. and Bouchard, D. 2013. Colloidal properties and stability of graphene oxide nanomaterials in the aquatic environment. Environ. Sci. Technol., 47(12): 130.

Deng, L. and Shi, Z. 2015. Synthesis and characterization of a novel Mg-Al hydrotalcite-loaded kaolin clay and its adsorption properties for phosphate in an aqueous solution. J. Alloys Comp., 637: 188-196.

Haouti, R.E., Ouachtak, H., Guerdaoui, A.E., Amedlous, A., Amaterz, E., Haounati, R., Addi, A. A., Akbal, F., Alem, N.E. and Taha, M.L. 2019. Cationic dye adsorption by Na-montmorillonite nano clay: Experimental study combined with a theoretical investigation using DFT-based descriptors and molecular dynamics simulations. J. Mol. Liq., 290: 111139.

He, G., Wang, C., Cao, J., Fan, L., Zhao, S. and Chai, Y. 2019. Carboxymethyl chitosan-kaolinite composite hydrogel for efficient copper ions trapping. J. Environ. Chem., 16: 541-563.

Hu, R., Dai, S., Shao, D., Alsaedi, A., Ahmad, B. and Wiang, X. 2015. Efficient removal of phenol and aniline from aqueous solutions using graphene oxide/polypyrrole composites. J. Mol. Liq., 203: 80-89.

Hussain, S.T. and Ali, S.A.K. 2021. Removal leads Pb (II) from wastewater using kaolin clay. IOP Conf. Series Mater. Sci. Eng., 1058(1): 012069.

layda, D., Duygu, E., Ali and Reza, K. 2016. Graphene oxides for removal of heavy and precious metals from wastewater. J. Mater. Sci., 14: 31.

Jing, J.H., Wu, H.Y., Shao, Y.W., Qi, X.D. and Wang, Y. 2019. Melamine foam-supported form-stable phase change materials with simultaneous thermal energy storage and shape memory properties for thermal management of electronic devices. ACS Appl. Mater. Interfaces, 11(21): 56.

Konkena, B. and Vasudevan, S. 2012. Understanding the aqueous dispersibility of graphene oxide and reduced graphene oxide through pKa measurements. J. Phys. Chem. Letts., 3(7): 867.

Kryuchkova, M. and Fakhrullin, R. 2018. Kaolin alleviates graphene oxide toxicity. . Environmental Science & Technology Letters. 5(5):295-300.

Li, J., Zhang, S., Chen, C., Zhao, G. and Wang, X. 2012. Removal of Cu(II) and fulvic acid by graphene oxide nanosheets decorated with Fe3O4 nanoparticles. ACS Appl. Mater. Interfaces, 4(9): 4991.

Liao, K.H., Lin, Y.S., Macosko, C.W. and Haynes, C.L. 2011. Cytotoxicity of graphene oxide and graphene in human erythrocytes and skin fibroblasts. Acs Appl. Mater. Interfaces, 3(7): 2607-2615.

Littunen, K., Hippi, U., Johansson, L.S., Sterberg, M., Tammelin, T., Laine, J. and Seppl J. 2011. Free radical graft copolymerization of nanofibrillated cellulose with acrylic monomers. Carbohydrate Polymers, 84(3): 1039-1047.

Mouni, L., Belkhiri, L., Bollinger, J.C., Bouzaza, A., Assadi, A., Tirri, A., Dahmoune, F., Madani K. and Remini, H. 2017. Removal of Methylene Blue from aqueous solutions by adsorption on Kaolin: Kinetic and equilibrium studies. Appl. Clay Sci., 153: 38-45.

Nandi, B.K., Goswami, A. and Purkait, M.K. 2009. Adsorption characteristics of brilliant green dye on kaolin. J. Hazard. Mater., 161(1): 387-395.

Nguyen, P. H., Le, Q.T., Pham, T.C.T. and Le, T.T. 2021. Synthesis of glue-free naa zeolite granules from natural kaolin for the adsorption of Pb(II) ions in aqueous solution using a fixed-bed column study. ACS Omega, 6(32): 21024-21032.

Pawar, R.R., Lalhmunsiama, G.P., Sawant, S.Y., Shahmoradi, B. and Lee, S.M. 2018. Porous synthetic hectorite clay-alginate composite beads for effective adsorption of methylene blue dye from an aqueous solution. Int. J. Biol. Macromol., 11: 1315.

Puri, C. and Sumana, G. 2018. Highly effective adsorption of crystal violet dye from contaminated water using graphene oxide intercalated montmorillonite nanocomposite. Appl. Clay Sci., 166(12): 102-112.

Qi, Z., Zhang, L. and Chen, W. 2014a. Transport of graphene oxide nanoparticles in saturated sandy soil. Environ. Process Impacts, 16(10): 2268-2277.

Qi, Z., Zhang, L., Wang, F., Hou, L. and Chen, W. 2014b. Factors controlling transport of graphene oxide nanoparticles in saturated sand columns. Environ. Toxicol. Chem., 33(5): 998-1004.

Queiroga, L.N.F., Pereira, M.B.B., Silva, L.S., Silva, F.E.C., Santos, I.M.G., Fonseca, M.G., Georgelin, T. and Jaber, M. 2019. Microwave bentonite silylation for dye removal: Influence of the solvent. Appl. Clay Sci., 168(2): 478-487.

Vallabani, N.V.S., Mittal, S., Shukla, R.K., Pandey, A.K., Dhakate, S.R., Pasricha, R. and Dhawan, A. 2011. Toxicity of graphene in normal human lung cells (BEAS-2B). J. Biomed. Nanotechnol., 7(1): 106.

Vimonses, V., Lei, S., Jin, B., Chow, C.W.K. and Saint, C. 2009. Adsorption of congo red by three Australian kaolins. Appl. Clay Sci., 43(3-4): 465-472.

Wang, C., Luo, H., Zhang, Z., Wu, Y., Zhang, J. and Chen, S. 2014. Removal of As(III) and As(V) from aqueous solutions using nanoscale zero-valent iron-reduced graphite oxide modified composites. J. Hazard. Mater., 268(15): 124-131.

Wang, J., Wang, X., Tan, L., Chen, Y., Hayat, T., Hu, J., Alsaedi, A., Ahmad, B., Guo, W. and Wang, X.. 2016. Performances and mechanisms of Mg/Al and Ca/Al layered double hydroxides for graphene oxide removal from aqueous solution. Chem. Eng. J., 297: 106-115.

Wiem, H., Nesrine, D., Bel, H., Hadjltaief, M. and Eloussaief, M.B. 2018. Sono-assisted adsorption of Cristal Violet dye onto Tunisian Smectite Clay: Characterization, kinetics, and adsorption isotherms. Ecotoxicol. Environ. Safety, 11: 235

Xing, M., Zhuang, S. and Wang, J. 2019. Efficient removal of Cs(I) from aqueous solution using graphene oxide. Prog. Nucl. Energy, 119: 103167.

Yavuz, O. and Saka, C. 2013. Surface modification with cold plasma application on kaolin and its effects on the adsorption of methylene blue. Appl. Clay Sci., 85(11): 96-102.

Yu, X., Tong, S., Ge, M., Zuo, J. and Song, W. 2012. One-step synthesis of magnetic composites of cellulose@iron oxide nanoparticles for arsenic removal. J. Mater. Chem. A, 3: 959-965

Zhang, S., Zeng, M., Li, J., Li, J., Xu, J. and Wang, X. 2014. Porous magnetic carbon sheets from biomass as an adsorbent for the fast removal of organic pollutants from aqueous solution. J. Mater. Chem. A, 2(12): 4391-4397.

Zhang, X., Yin, J., Peng, C., Hu, W., Zhu, Z., Li, W., Fan, C. and Huang, Q. 2011. Distribution and biocompatibility studies of graphene oxide in mice after intravenous administration. Carbon, 49(3): 986-995.

Zong, P., Wang, S., Zhao, Y., Wang, H. and He, C. 2013. Synthesis and application of magnetic graphene/iron oxides composite for the removal of U(VI) from aqueous solutions. Chem. Eng. J., 220: 45-52.

Zou, Y., Wang, X., Ai, Y., Liu, Y., Li, J., Ji, Y. and Wang, X., 2016. Coagulation Behavior of Graphene Oxide on Nanocrystallined Mg/Al Layered Double Hydroxides: Batch Experimental and Theoretical Calculation Study. Environ. Sci. Technol., 50(7): 3658.